

Electronic Supplementary Information for

Photoinduced Bimolecular Electron Transfer from Aromatic Amines to Pentafluorophenyl Porphyrin Combined with Ultrafast Charge Recombination Persistence with Marcus Inverted Region

*Yeduru Venkatesh^{1,2}, Venkatesan Munisamy¹, Bheerappagari Ramakrishna¹, Pippara
Hemant Kumar¹, Haraprasad Mandal¹, Prakriti Ranjan Bangal^{1,2*}*

¹ Inorganic and Physical Chemistry Division, CSIR-Indian Institute of Chemical Technology,
Uppal Road, Tarnaka, Hyderabad, 500007, India.

² Academy of Scientific and Innovative Research, 2-Rafi Marg, New Delhi, 110001, India.

* Corresponding author Email: prakriti@iict.res.in

Index

1. **Figure S1** Absorption spectra of H₂F₂₀TPP in DCM and AN solution
2. **Figure S2** Fluorescence spectra of H₂F₂₀TPP in DCM in three regions, S₂ Q_y and Q_x.
3. Diffusion and quenching parameters
4. Marcus theory and quenching parameters:
5. **Figure S3.** FUS decay profile of Q_x Fluorescence in 10 ps time window.
6. **Figure S4:** Change of amplitude of fastest decay component as function of amine concentration.
7. **Figure S5.** Change of characteristic time constant of third decay component (as function of Donor (amines) concentration
8. **Figure S6** Probe wavelength dependent time profile of transient absorption signals of H₂F₂₀TPP in presence of AN and or DMAN.
9. **Figure S7** Coherent effect in DMAN
10. **Figure S8** Comparison of data and fits of target model is reported, in the form of spectra at different selected delay times and kinetic traces at several selected wavelengths for H₂F₂₀TPP in DCM in absence of any donor.
11. **Figure S9A** 3D surface plot of TA spectra of H₂F₂₀TPP in DCM in presence of 0.1 M of AN, Comparison of data and fits of target model in the form of spectra at different selected delay times and kinetic traces at several selected wavelengths for H₂F₂₀TPP in DCM in presence of 0.1 molar AN.
Figure S9B. Comparison of data and fits of target model is reported, in the form of spectra at different selected delay times and kinetic traces at several selected wavelengths for H₂F₂₀TPP in DCM in presence of 0.1 molar AN.
12. **Figure S10A.** 3D surface plot of TA spectra of H₂F₂₀TPP in DCM in presence of 0.02 M of DMAN, Schematic kinetic model used for target analysis of TA data matrices of H₂F₂₀TPP in presence of 0.02 M DMAN, Estimated SADS of H₂F₂₀TPP in DCM in presence of 0.02 molar DMAN, Estimated population profile respective and Comparison of data and fits, in the form of spectra at different selected delay times and kinetic traces
Figure S10 B. Schematic kinetic model used for target analysis of TA data matrices of H₂F₂₀TPP in presence of 0.02 M DMAN upon 397 nm excitation. τ_1 , τ_2 , τ_3 , τ_4 , τ_5 and τ_6 are global lifetimes of the respective states. k_{10} , k_{12} , k_{13} , k_{20} , k_{23} , k_{30} , k_{34} , k_{35} , k_{40} , k_{45} , k_{46} and k_{60} are microscopic rate constants of the respective transitions. $k_{35}+k_{45}$ is the rate constant of CS state formation and k_{50} is the rate of charge recombination and they are identical to each other. The estimated rate constants and lifetime values are indicated in the figure at several selected.
Figure S10C. Estimated SADS of H₂F₂₀TPP in DCM in presence of 0.02 M of DMAN
Figure S10D Estimated population profile respective states of H₂F₂₀TPP in DCM in presence of 0.02 M of DMAN.

Figure S10E. Comparison of data and fits is reported, in the form of spectra at different selected delay times and kinetic traces at several selected wavelengths for $H_2F_{20}TPP$ in DCM in presence of 0.02 M of DMAN.

- 13. Figure S11A.** 3D surface plot of TA spectra of $H_2F_{20}TPP$ in neat AN, comparison of data and fits in the form of spectra at different selected delay times and kinetic traces at several selected wavelengths.

Figure S11B. Comparison of data and fits of target model is reported, in the form of spectra at different selected delay times and kinetic traces at several selected wavelengths for $H_2F_{20}TPP$ in neat AN. Time in logarithmic scale.

- 14. Figure S12** 3D surface plot of TA spectra of $H_2F_{20}TPP$ in neat DMAN
- 15. Figure S13:** Schematic kinetic model used for target analysis of TA data matrices of $H_2F_{20}TPP$ in neat DMAN
- 16. Figure S14.** Spectra at different time and temporal profile at different wavelength of $H_2F_{20}TPP$ in neat DMAN
- 17. Figure 15.** Estimated species associated difference spectra (SADS) of $H_2F_{20}TPP$ in neat DMAN arising out of target analysis and the population profiles of respective states/compartments .

Figure S1 Absorption spectra of H₂F₂₀TPP in DCM and AN solution. Inset shows the magnified view of Q band region.

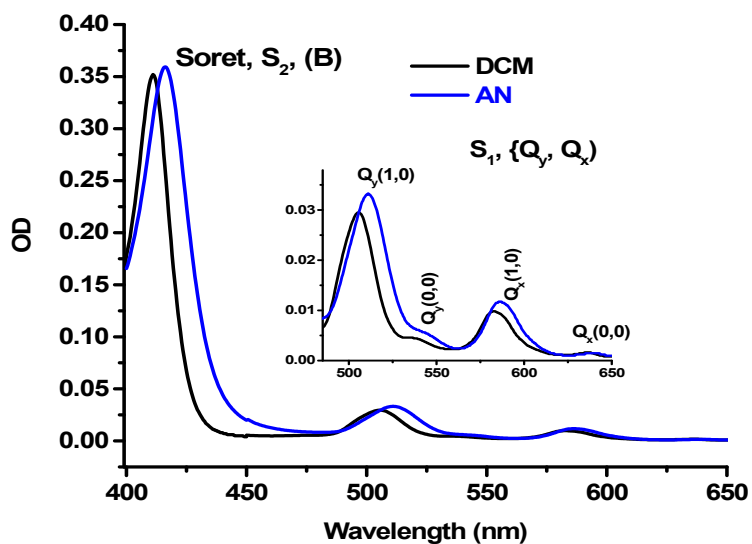
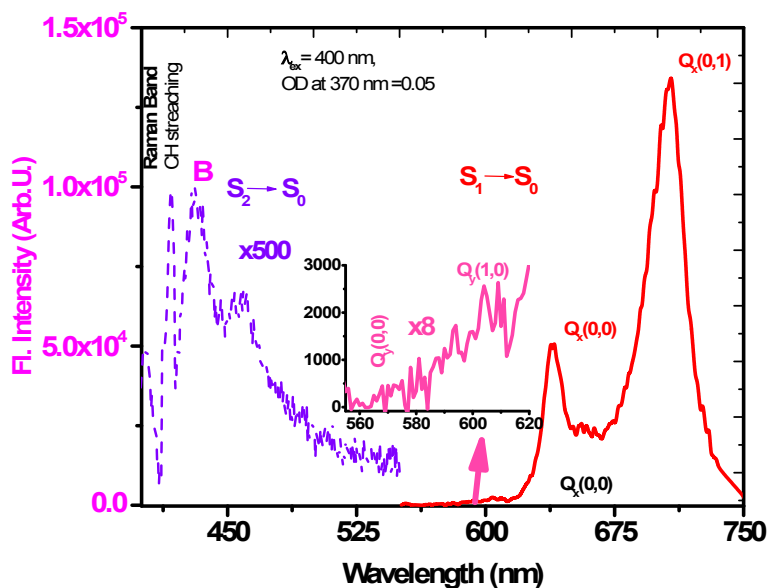


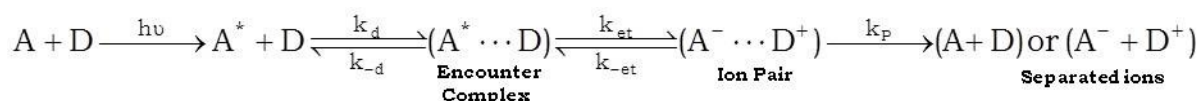
Figure S2. Fluorescence spectra of H₂F₂₀TPP in DCM in three regions, S₂ Q_y and Q_x.



Diffusion and quenching parameters

PET occurs from ground state donor to excited state acceptor and is rationalized by the free energy change (ΔG^0) for the ET reaction. Scheme 1 is presented to explain the observed ET phenomenon in the H₂F₂₀TPP- Anilines pair system.

Scheme 1



According to the scheme, excited state acceptor (A^*) and the ground state donor molecules diffuse together to form an encounter complex, ($A^* \cdots D$). The encounter complex then undergoes reorganization to form the transition state, where ET occurs from donor to acceptor to form an ion pair state ($A^- \cdots D^+$). The relevant parameters, k_d and k_{-d} are the diffusion-controlled rate constants for the formation and dissociation of the encounter complex ($A^* \cdots D$), k_{et} and k_{-et} are the forward and backward ET rate constants and k_p is the sum of all the rate constants which causes the disappearance of ion pairs. After the formation of ion pair, it may revert back to uncharged molecules (charge recombination (k_{CR})) or form charge separated ion pair (solvent separated ions (A^- and D^+)). Following this assumption and applying steady-state approximation, the observed bimolecular quenching constant can be derived as follows

$$\frac{1}{k_q} = \frac{1}{k_d} + \frac{1}{Kk_{et}} \quad (1)$$

where $K(k_d/k_{-d})$ is the diffusional equilibrium constant for the encounter complex formation and can be estimated using Fuoss–Eigen model.¹

$$K = \frac{4}{3} \pi R_{DA}^3 N_A \exp\left(\frac{e^2}{4\pi\epsilon\epsilon_0 k T R_{DA}}\right) 1000 \quad (2)$$

In Eq. 4.5, N_A is the Avogadro's number, R_{DA} is the centre to centre distance between donor and acceptor in the encounter complex. For neutral molecules diffusion occurs freely in homogeneous solution and the exponential term vanishes reducing the Eq. 4.55 to Eq. 4.66

$$K = \frac{4}{3} \pi R_{DA}^3 N_A 1000 \quad (3)$$

Thus taking the different donor acceptor distances, values for K are estimated for all donor-acceptor pairs and which are in the range of 1.6 to 2.35 mol⁻¹ dm³ for the present H₂F₂₀TPP-amine system. Also the diffusion coefficient (D) of the reactants were calculated following Stokes-Einstein equation 4, from which the diffusion controlled rate constants (k_d) by can be calculated using equation 5

$$D = \frac{k_B T}{6 \pi \eta r} \quad (4)$$

where k is the Boltzmann constant and η (0.423 cp) is the kinematic viscosity of DCM at 298 K and r is the radii of the molecules. Taking the said radii of respective donors and acceptor, the diffusion coefficient for each donor acceptor pairs ($D_{AD} = D_A + D_D$, diffusion coefficient of donor (D_D), diffusion coefficient acceptor (D_A)) are calculated at room temperature and listed in Table S1 (main text). In steady state picture, time independent Smoluchowski equation (Eq. 5) is used to calculate the diffusion controlled rate constant, where N_A is the Avogadro number. The k_d and k_{et} values were calculated at room temperature for all donor-acceptor systems and shown in Table 4.2.

$$k_d = 4 \pi R_{DA} N_A D_{DA} * 10^3 \quad (5)$$

Table S1: Estimated diffusion coefficients, rate constants, reorganizational energies, free energy changes, activation energies and frequency factors for different aromatic amine-H₂F₂₀TPP pairs.

Anilines	$D_{DA} \cdot 10^9$	$k_d \cdot 10^{-10}$	$k_q \cdot 10^{-9}$	$k_{et} \cdot 10^{-9}$	λ^a	λ_s^b	λ_{in}	$-\Delta G^0$	ΔG^*
	m^2s^{-1}	$M^{-1}s^{-1}$	$M^{-1}s^{-1}$	s^{-1}	(eV)	(eV)	(eV)	(eV)	(eV)
AN	2.63	1.75	2.8	2.05	1.1	0.87	0.14	0.29	0.04
MAN	2.34	1.66	3.7	2.40	1.31	0.88	0.43	0.50	0.03
EAN	2.25	1.64	3.9	2.42	1.30	0.83	0.47	0.52	0.04
DMAN	2.36	1.67	5.9	4.60	1.32	0.87	0.45	0.56	0.02
DEAN	2.18	1.62	5.8	4.5	1.32	0.78	0.54	0.60	0.02

Marcus theory and quenching parameters:

In general, activation controlled ET rate constant can be expressed by an Arrhenius type of equation¹ given by equation 5.

$$k_{et} = A \left(\frac{-\Delta G^*}{k_B T} \right) \quad (6)$$

where $A(10^{10} s^{-1})$ is the frequency factor and ΔG^* is the free energy of activation for the ET process. Further, activation energy can be obtained from quadratic relation (Eq. 6) derived by Marcus which has been extensively been used for a variety of ET reactions.

$$\Delta G^* = \frac{(\Delta G^0 + \lambda)^2}{4\lambda} \quad (7)$$

ΔG^0 is the free energy change for the ET reaction and λ is total reorganization energy. Using Eq. 6 & 6, ΔG^* and λ values were calculated respectively and the obtained values are

tabulated in Table 1. The total reorganization energy which is about 1 eV and it is found to be bigger than the thermodynamic free energy i.e. $-\Delta G < \lambda$ for all cases. The rate constant increases with increasing free energy of reaction, indicating that the ET process in the present D-A system falls in Marcus normal region.

Total reorganization energy is partitioned into two components which is a sum of internal reorganization energy (λ_{in}) and solvent reorganization energy (λ_s).

$$\lambda = \lambda_s + \lambda_{in} \quad (8)$$

Considering a non equilibrium polarization of the medium and employing the dielectric continuum model for the solvent, Marcus derived the following expression for λ_s .³²

$$\lambda_s = \frac{e^2}{4\pi\epsilon_0} \left\{ \frac{1}{2r_D} + \frac{1}{2r_A} - \frac{1}{2R_{DA}} \right\} \left\{ \frac{1}{n^2} - \frac{1}{\epsilon} \right\} \quad (9)$$

where r_D and r_A is the radius of the donor and acceptor respectively, R_{DA} is the separation between the donor and acceptor in the encounter complex, n is the refractive index and ϵ is the dielectric constant of the solvent. Thus λ_s is obtained by inserting the relevant values into Eq. 9, and finally λ_{in} is calculated from Eq. 8 for all the donor-acceptor pairs and listed in Table 1. The λ_{in} values obtained are in between 0.08 - 0.49 eV, which is in the range normally observed for organic systems.³ The present results also indicate that the solvent reorganization has a major contribution to the total reorganization required for the ET to take place under the diffusive conditions.

1. J. M. Chen, T. I. Ho and C. Y. Mou, *J Phys Chem*, 1990, **94**, 2889.
2. R. A. Marcus and N. Sutin, *Biochim Biophys Acta*, 1985, **811**, 265.
3. H. Heitele, F. Pollinger, T. Haberle, M. E. Michel beyerle and H. A. Staab, *J Phys Chem*, 1994, **98**, 7402.

Figure S3. FUS decay profiles of Qx Fluorescence of H2F20TPP measured at 640 nm in DCM solution as function of amine concentration, ($\lambda_{EX} = 397$ nm). (A),(B),(C) represent 10 ps time domain and (D) shows 100 ps time domain

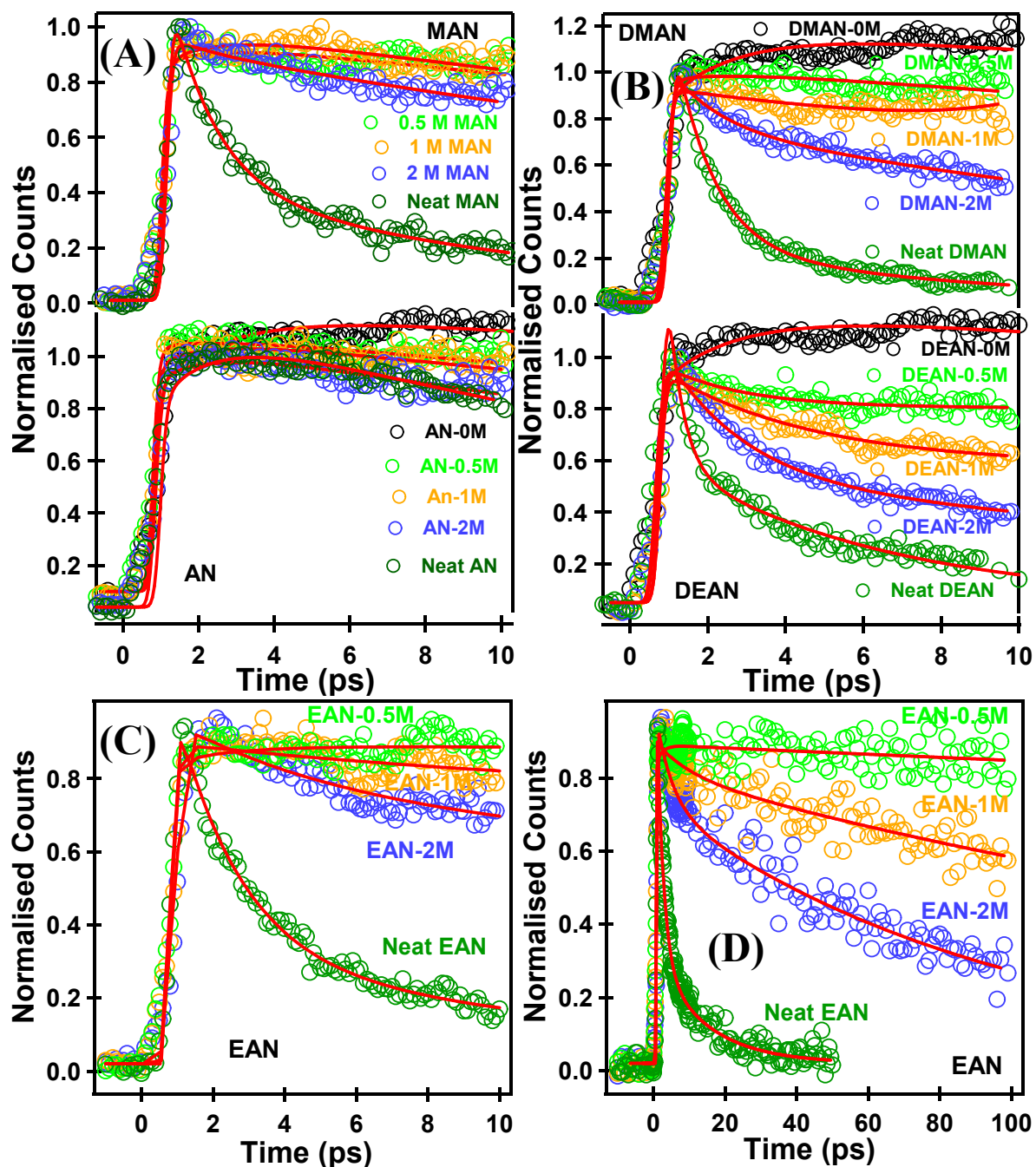


Figure S4: Change of amplitude of fastest decay component as function of amine concentration obtained from fluorescence up-conversion data at 640 nm emission wavelength upon excitation at 397 nm. Solid lines are first order exponential fit.

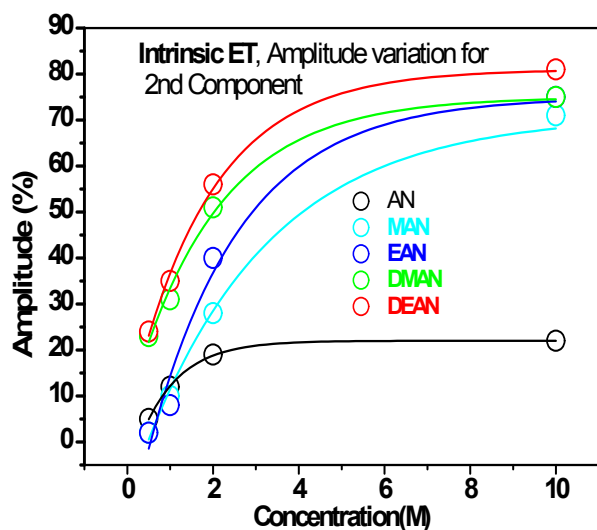


Figure S5: Change of characteristic time constant of third decay component (as function of Donor (amine) concentration) obtained from fluorescence up-conversion data at 640 nm emission wavelength when excited at 397 nm. Solid lines are first order exponential fit.

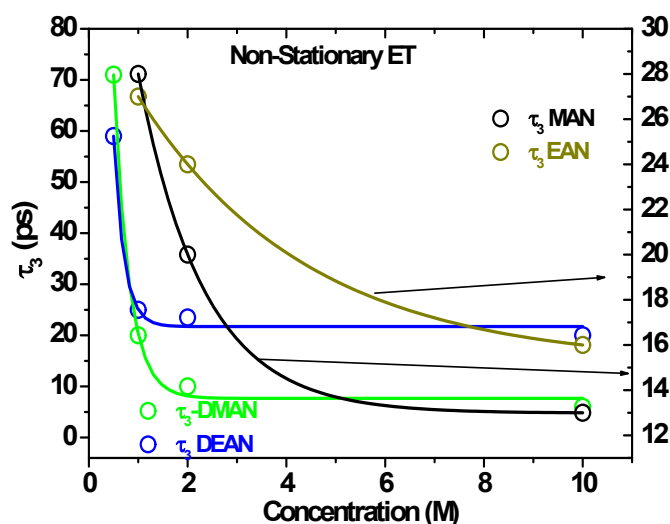


Figure S6 Probe wavelength dependent time profile of transient absorption signals of $H_2F_{20}TPP$ in presence of different concentration of AN and DMAN.

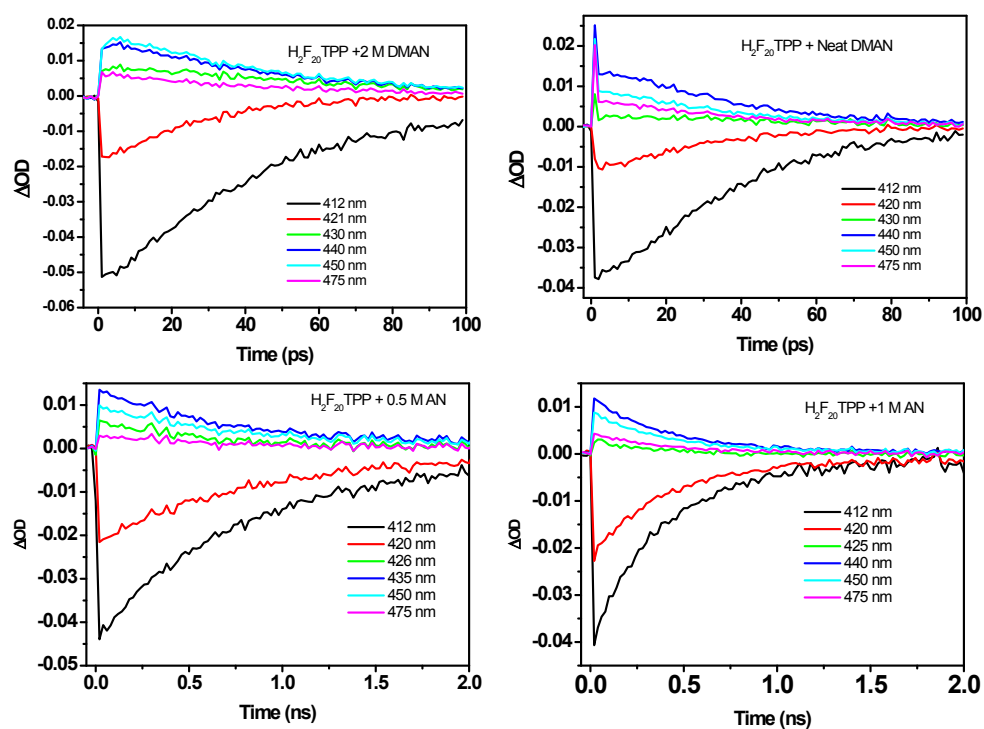


Figure S7 Coherent effect in DMAN

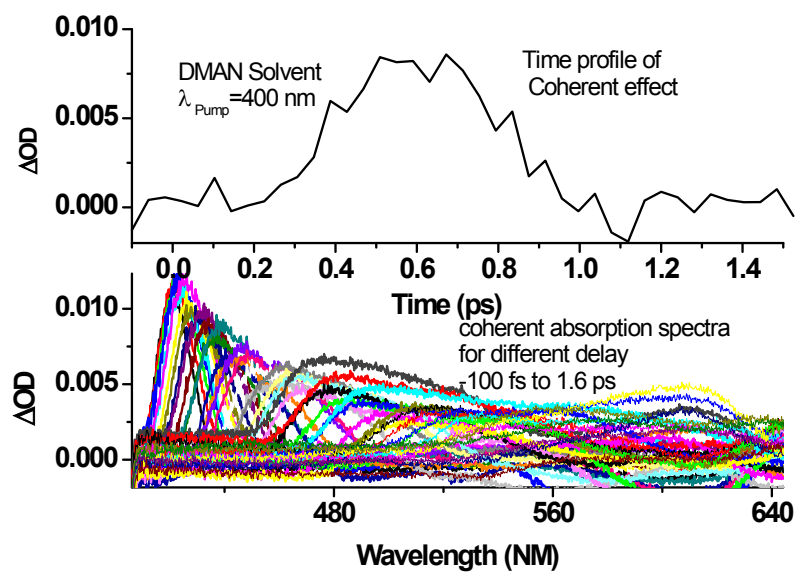


Figure S8 Comparison of data and fits of target model is reported, in the form of spectra at different selected delay times and kinetic traces at several selected wavelengths for $\text{H}_2\text{F}_{20}\text{TPP}$ in DCM in absence of any donor.

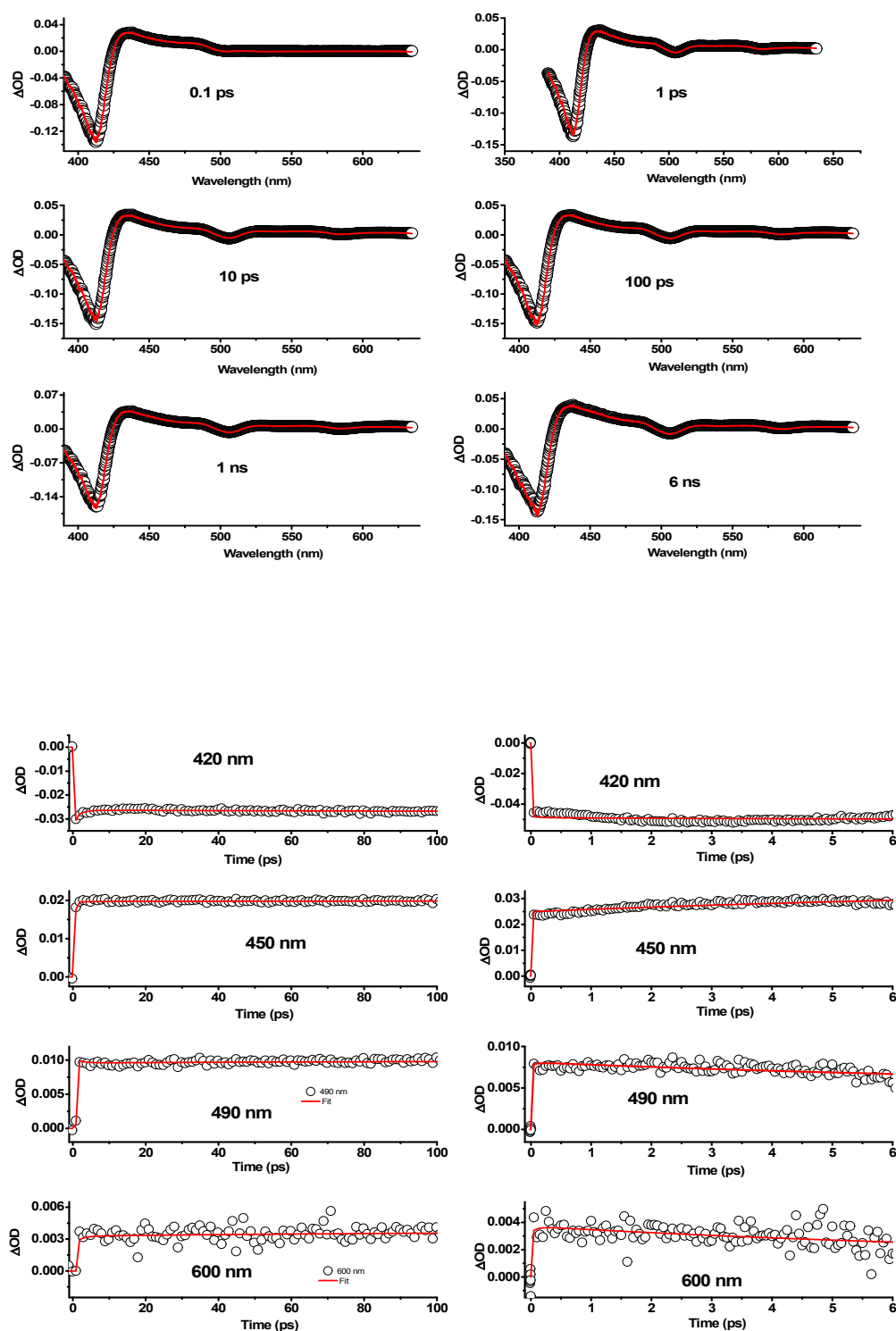


Figure S9A 3D surface plot of TA spectra of $\text{H}_2\text{F}_{20}\text{TPP}$ in DCM in presence of 0.1 M of AN, X axis represent time, Y-axis represents wavelength and Z-axis represent ΔOD , X-Y surface shows the heat map of ΔOD of TA spectra and As indicated in the color map, the zero level is colored in red, dark red indicates positive signals (i.e., photoinduced absorption), and yellow/blue denote negative signals (i.e., decrease in absorption due to stimulated emission and/or ground-state photobleaching.). Upper panel represent TA spectra in 100 ps time window, lower panel is for 2 ns time window. Two representative TA spectra (at 1 and 100 ps for top panel, 0.02 and 2 ns for lower panel) are shown in Y-Z plane and two temporal profile (at 415 and 440 nm) are shown in X-Z plane.

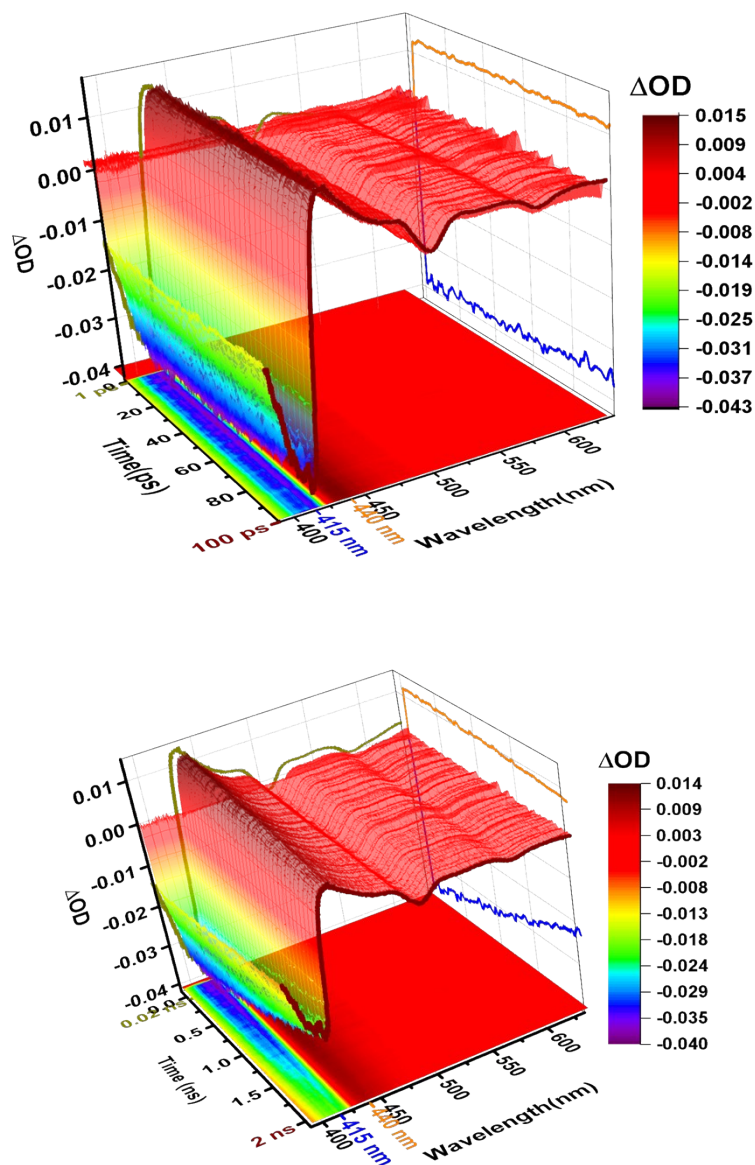


Figure S9B. Comparison of data and fits of target model is reported, in the form of spectra at different selected delay times and kinetic traces at several selected wavelengths for $\text{H}_2\text{F}_{20}\text{TPP}$ in DCM in presence of 0.1 molar AN.

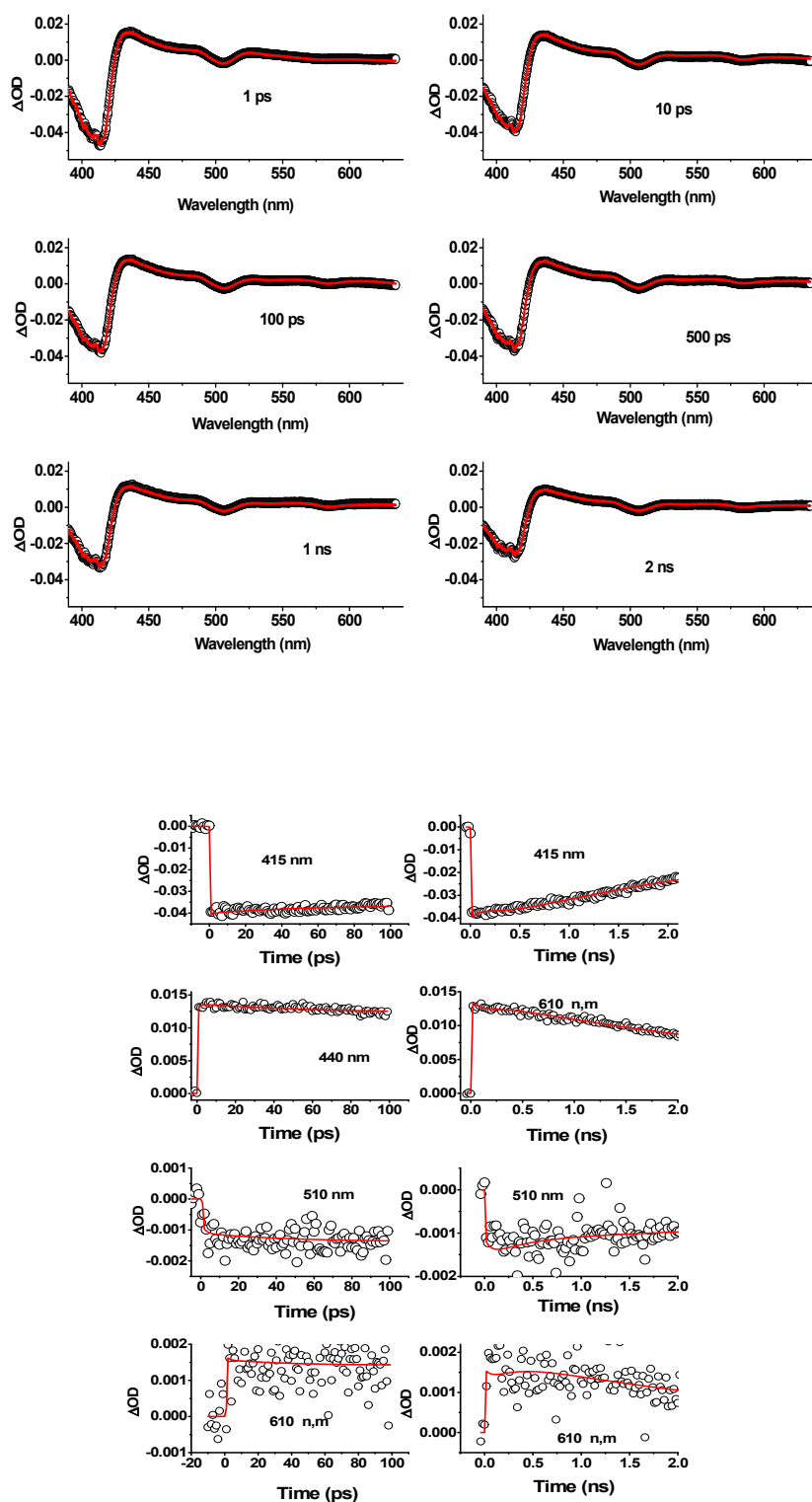


Figure S10A. 3D surface plot of TA spectra of H₂F₂₀TPP in DCM in presence of 0.02 M of DMAN, X axis represent time, Y-axis represents wavelength and Z-axis represent ΔOD , X-Y surface shows the heat map of ΔOD of TA spectra and As indicated in the color map, the zero level is colored in red, dark red indicates positive signals (i.e., photoinduced absorption), and yellow/blue denote negative signals (i.e., decrease in absorption due to stimulated emission and/or ground-state photobleaching.). Upper panel represent TA spectra in 100 ps time window, lower panel is for 2 ns time window. Two representative TA spectra (at 1 and 100 ps for top panel, 0.1 and 2 ns for lower panel) are shown in Y-Z plane and two temporal profile (at 415 and 440 nm) are shown in X-Z plane.

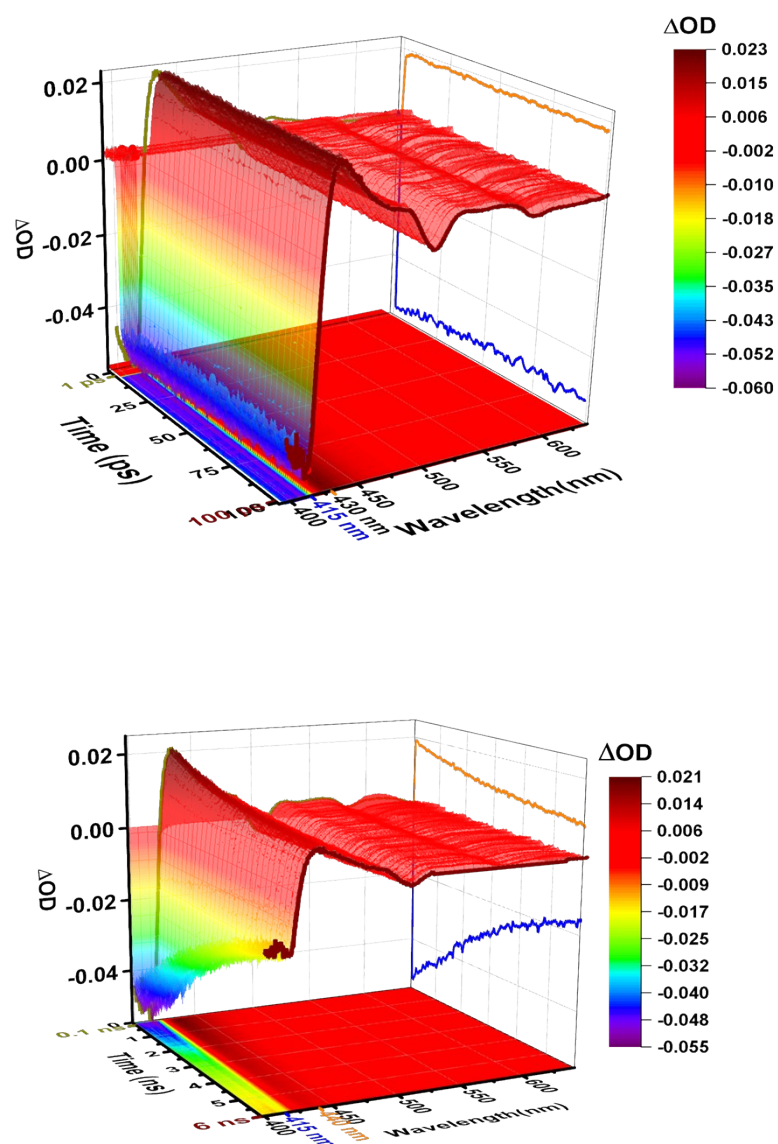


Figure S10 B. Schematic kinetic model used for target analysis of TA data matrices of H₂F₂₀TPP in presence of 0.02 M DMAN upon 397 nm excitation. τ_1 , τ_2 , τ_3 , τ_4 , τ_5 and τ_6 are global lifetimes of the respective states. k_{10} , k_{12} , k_{13} , k_{20} , k_{23} , k_{30} , k_{34} , k_{35} , k_{40} , k_{45} , k_{46} and k_{60} are microscopic rate constants of the respective transitions. $k_{35}+k_{45}$ is the rate constant of CS state formation and k_{50} is the rate of charge recombination and they are identical to each other. The estimated rate constants and lifetime values are indicated in the figure.

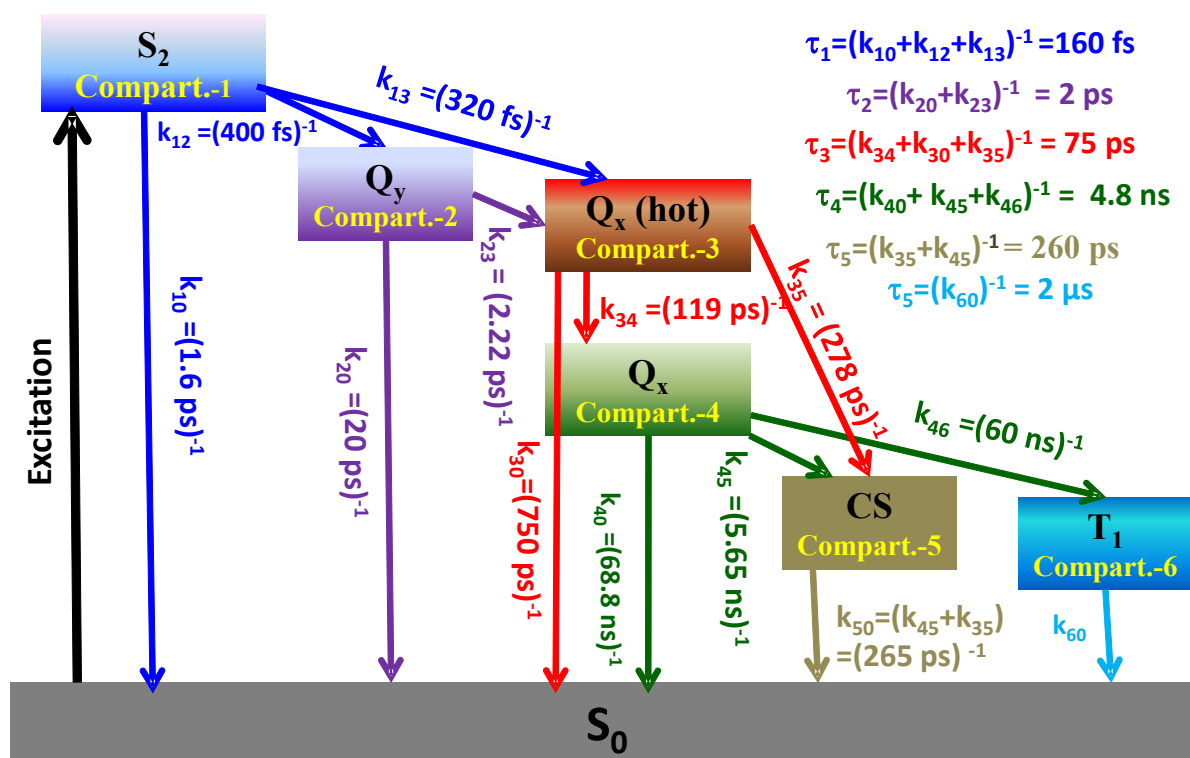


Figure S10C. Estimated SADS of H₂F₂₀TPP in DCM in presence of 0.02 M of DMAN

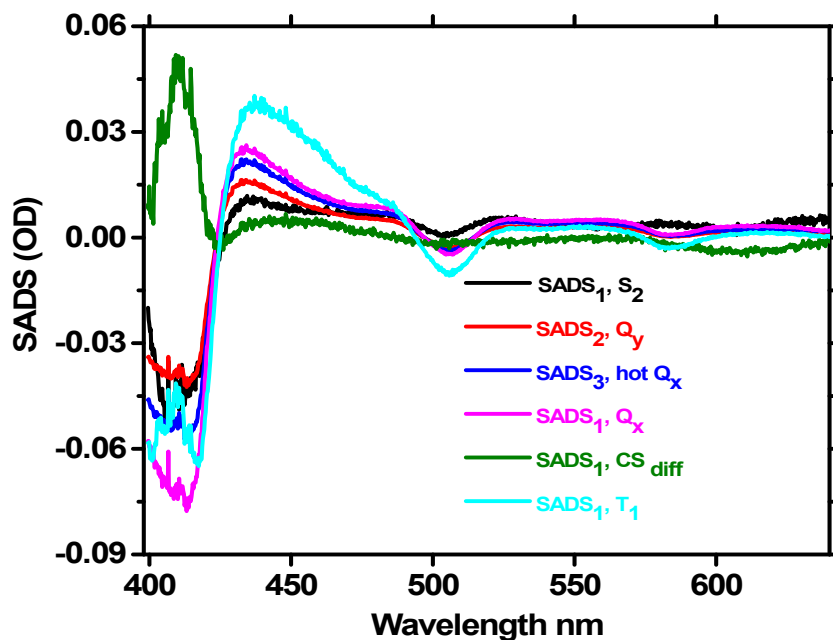


Figure S10D Estimated population profile respective states of H₂F₂₀TPP in DCM in presence of 0.02 M of DMAN.

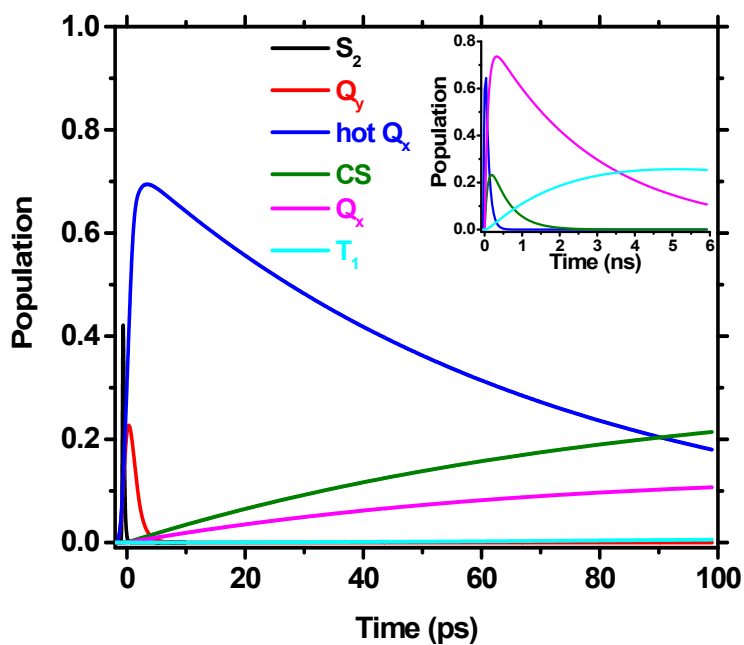


Figure S10E. Comparison of data and fits is reported, in the form of spectra at different selected delay times and kinetic traces at several selected wavelengths for $\text{H}_2\text{F}_{20}\text{TPP}$ in DCM in presence of 0.02 M of DMAN.

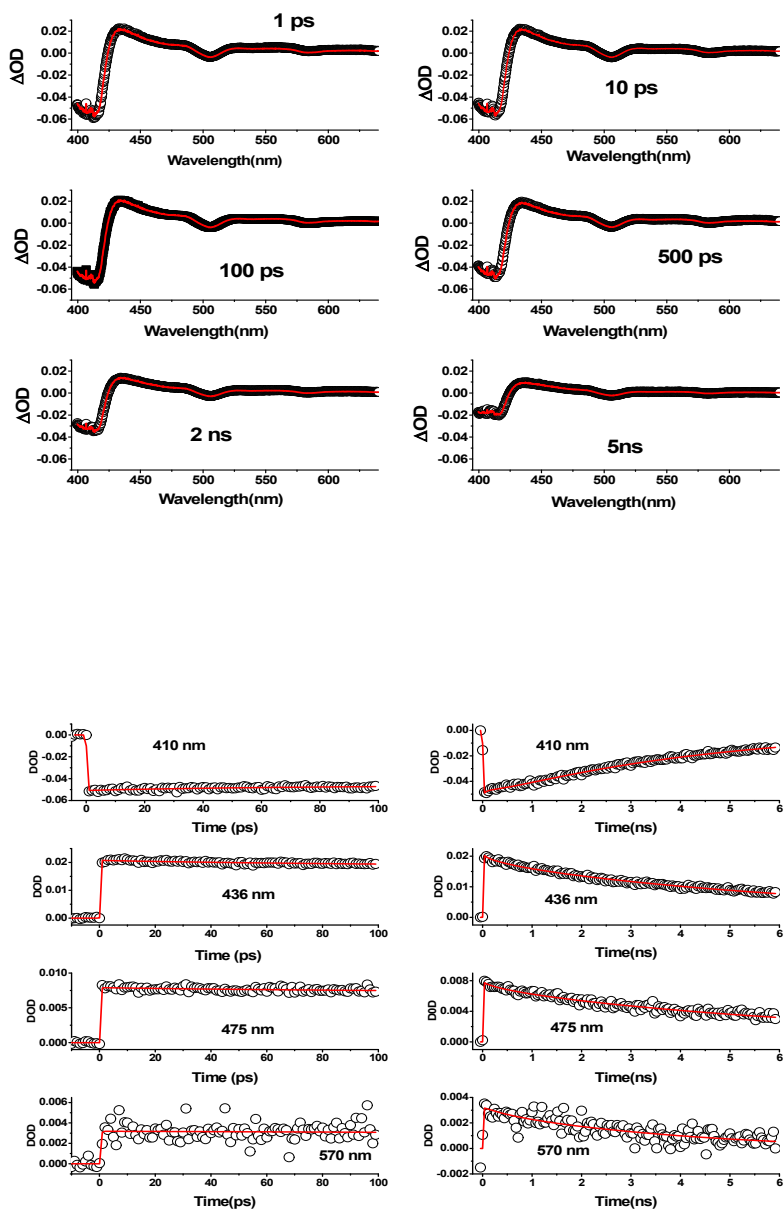


Figure S11A. 3D surface plot of TA spectra of H₂F₂₀TPP in neat AN, X axis represents time, Y-axis represents wavelength and Z-axis represents ΔOD , X-Y surface shows the heat map of ΔOD of TA spectra and As indicated in the color map, the zero level is colored in reddish yellow, red/dark red indicates positive signals (i.e., photoinduced absorption), and yellow/blue denote negative signals (i.e., decrease in absorption due to stimulated emission and/or ground-state photobleaching.). Two representative TA spectra at 1 and 100 ps are shown in Y-Z plane and two temporal profile at 415 and 450 nm are shown in X-Z plane

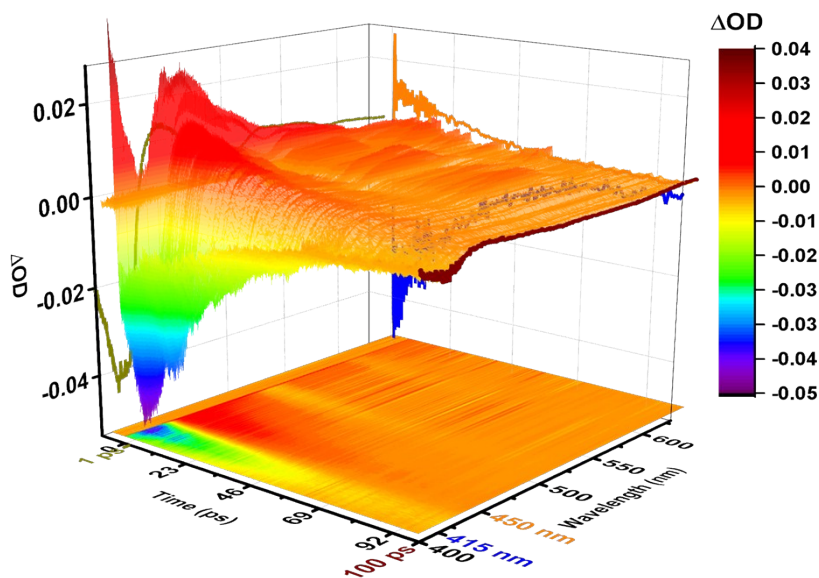
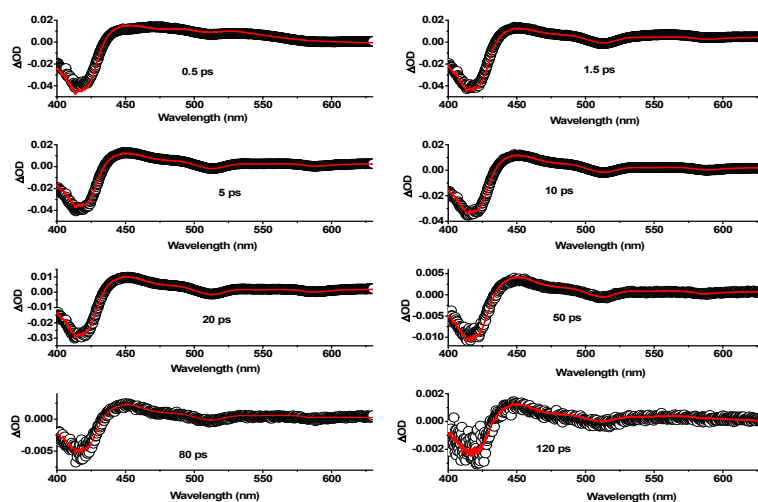


Figure S11B. Comparison of data and fits of target model is reported, in the form of spectra at different selected delay times and kinetic traces at several selected wavelengths for H₂F₂₀TPP in neat AN. Time in logarithmic scale.



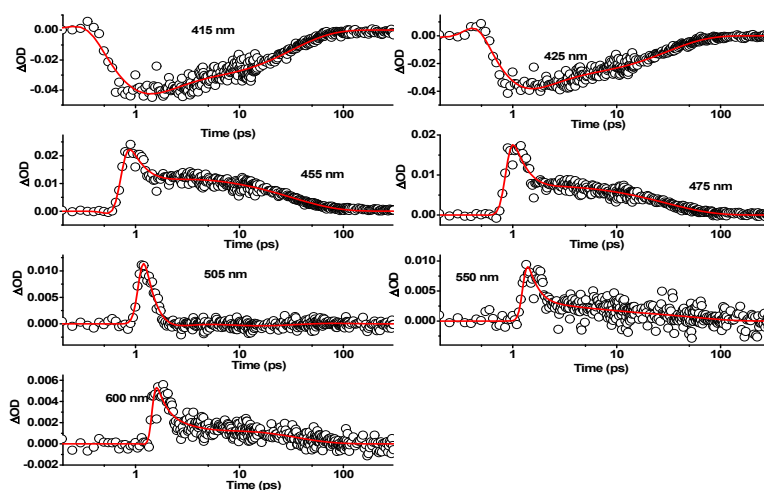


Figure S12 3D surface plot of TA spectra of $\text{H}_2\text{F}_{20}\text{TPP}$ in neat DMAN, X axis represents time, Y-axis represents wavelength and Z-axis represents ΔOD , X-Y surface shows the heat map of ΔOD of TA spectra and As indicated in the color map, the zero level is colored in reddish yellow, red/dark red indicates positive signals (i.e., photoinduced absorption), and yellow/blue denote negative signals (i.e., decrease in absorption due to stimulated emission and/or ground-state photobleaching.). Two representative TA spectra at 1 and 100 ps are shown in Y-Z plane and two temporal profile at 415 and 450 nm are shown in X-Z plane.

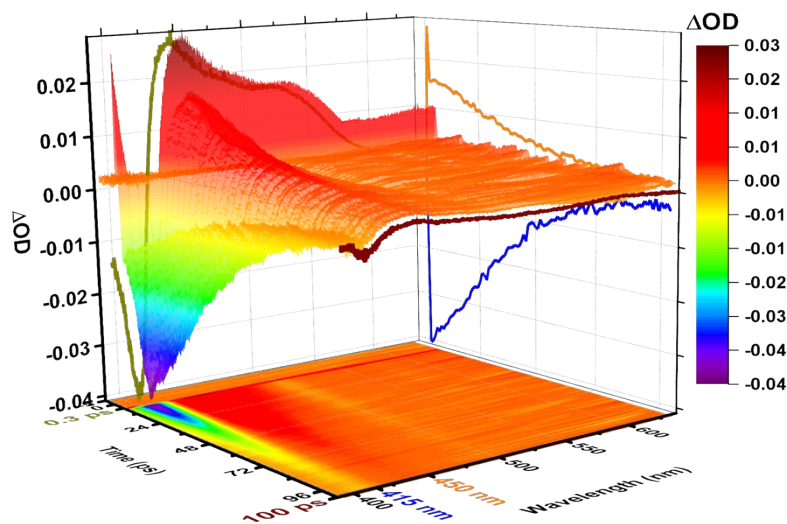


Figure S13: Schematic kinetic model used for target analysis of TA data matrices of H₂F₂₀TPP in neat DMAN upon 397 nm excitation. $\tau_1, \tau_2, \tau_3, \tau_4, \tau_5$ and τ_6 are global lifetimes of the respective states. $k_{10}, k_{12}, k_{13}, k_{20}, k_{23}, k_{24}, k_{30}, k_{34}, k_{35}, k_{40}$, and k_{50} are microscopic rate constants of the respective transitions. k_{24} is the rate constant of CS_i state formation and k_{40} is the rate of charge recombination with equal value to that of k_{24} , similarly, k_{35} the rate constant of CS_{non} state formation and k_{50} is the rate of charge recombination and they are identical to each other. The estimated rate constants and lifetime values are indicated in the figure.

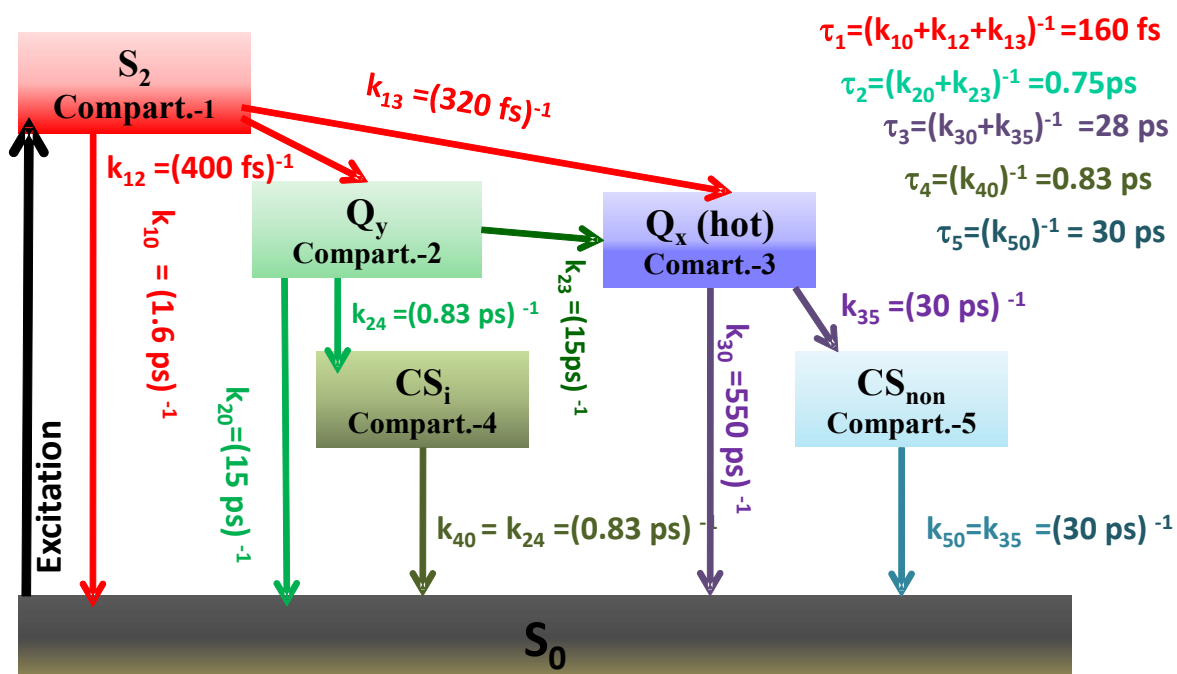


Figure S14. Spectra at different time and temporal profile at different wavelength of H₂F₂₀TPP in neat DMAN

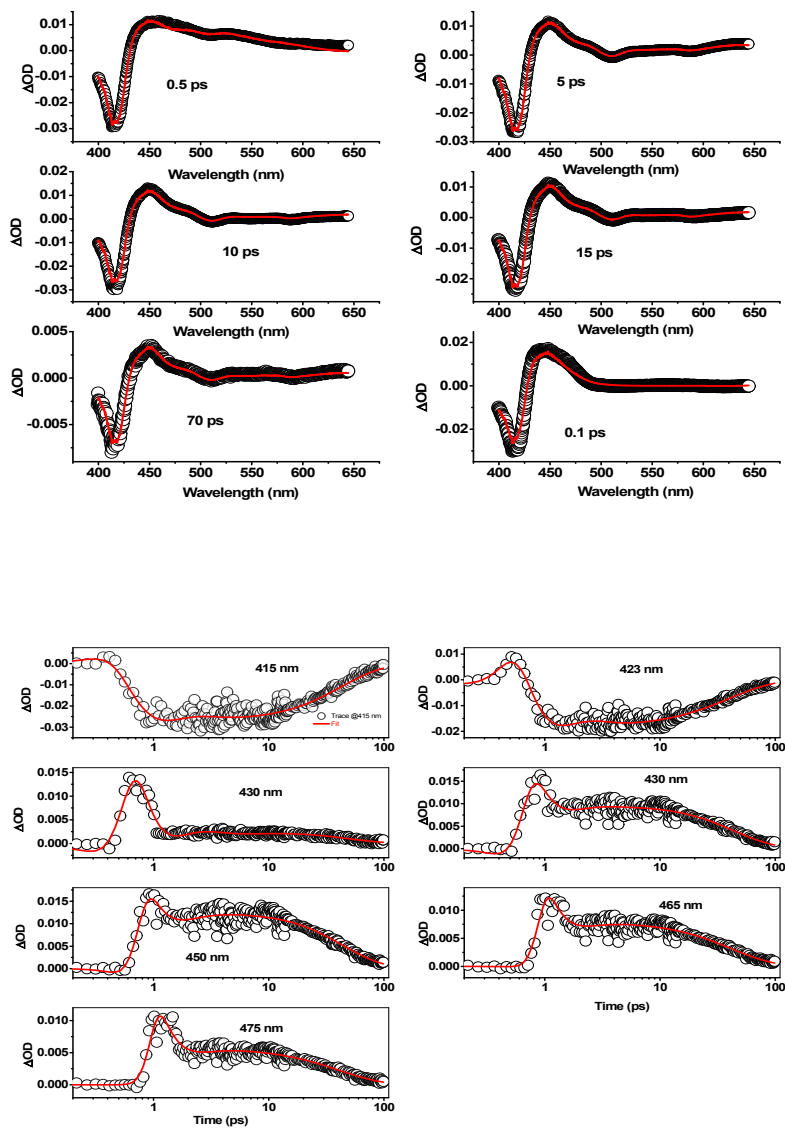


Figure S15. Estimated species associated difference spectra (SADS) of $H_2F_{20}TPP$ in neat DMAN arising out of target analysis (A) and the population profiles of respective states/ compartments (B), Inset in (B) are population profiles in 10 ps window.

